THESIS FOR THE DEGREE OF LICENTIATE OF ENGINEERING IN SOLID AND STRUCTURAL MECHANICS

Surface defects in rails

Potential influence of operational parameters on squat initiation

ROBIN ANDERSSON

Department of Applied Mechanics
CHALMERS UNIVERSITY OF TECHNOLOGY

Göteborg, Sweden 2015

Surface defects in rails
Potential influence of operational parameters on squat initiation
ROBIN ANDERSSON

Thesis for the degree of Licentiate of Engineering 2015:12
ISSN 1652-8565
Department of Applied Mechanics
Chalmers University of Technology
SE-412 96 Göteborg
Sweden
Telephone: +46 (0)31-772 1000

Chalmers Reproservice
Göteborg, Sweden 2015

Surface defects in rails
Potential influence of operational parameters on squat initiation
Thesis for the degree of Licentiate of Engineering in Solid and Structural Mechanics
ROBIN ANDERSSON
Department of Applied Mechanics
Chalmers University of Technology

Abstract

Despite significant efforts throughout the last decades, the mechanisms behind the formation of squats — a form of rolling contact fatigue (RCF) damage in rails — are not fully understood. Proposed causes of initiation involve, but are not limited to, small initial rail surface irregularities which yield high contact stresses, rail corrugation and varying friction conditions. To complicate matters further, a very similar rail defect — the stud — has started to appear during the last ten years. This defect lacks common signs of RCF initiated damage, such as large scale plastic deformations, and is commonly found in connection with so-called white etching layers.

The first paper of this thesis (Paper A) concerns a simplified two-dimensional model which is used to evaluate the dynamic interaction between a train and a flexible track. Wheel–rail contact stresses (and the resulting contact forces) are used to make assessments of the RCF impact due to rail surface irregularities under varying operational conditions. Excitation due to isolated rail defects and rail corrugation are considered. Differences in predicted RCF impact using a two-dimensional and a (computationally more expensive) three-dimensional contact model are investigated.

A computational framework for more detailed RCF assessment is also established (Paper B). Wheel–rail contact stresses from the dynamic vehicle–track model are used as prescribed loads imposed onto a refined continuum finite element model of a rail section. This makes it possible to compute resulting stress and strain fields in the rail material. The propensity of RCF initiation is quantified using accumulated strain and the Jiang–Sehitoglu fatigue parameter.

Finally (in Paper C), the aforementioned computational framework is utilised to perform detailed analyses of interesting operational scenarios that have been identified in Paper A. Further, the influence of interacting surface irregularities and varying friction conditions along the rail are investigated.

The aim of this thesis is to increase the knowledge regarding squat initiation by means of numerical modelling. Such an improved understanding of squat initiation will also be beneficial in order to understand and mitigate the corresponding form of damage occuring on wheels — so called RCF clusters.

Keywords: Rail surface irregularities; squats; rolling contact fatigue; dynamic vehicle–track interaction; rail corrugation;

Preface

This work has been carried out between April 2013 and May 2015 at the Department of Applied Mechanics at Chalmers University of Technology. It is conducted as a part of project MU31 — "Squats in rails and RCF clusters on wheels" within the Centre of Excellence CHARMEC (CHalmers Railway MEChanics).

I would like to thank my main supervisor Elena Kabo and co-supervisors Peter Torstensson, Anders Ekberg and Fredrik Larsson for their help and encouragement. This work would have been impossible without their continuous support. Furthermore, I would like to thank the members of the reference group for interesting discussions.

Gothenburg, May 2015
Robin Andersson

Thesis

This thesis consists of an extended summary and the following appended papers:

Paper A R. Andersson, P. T. Torstensson, E. Kabo and F. Larsson. The influence of rail surface irregularities on contact forces and local stresses. *Vehicle System Dynamics* **53**.1 (2015), 68–87.

Paper B R. Andersson, P. T. Torstensson, E. Kabo and F. Larsson. An efficient approach to analyse rail surface irregularities accounting for dynamic train–track interaction and inelastic deformations. *Submitted for international publication* (2015)

Paper C R. Andersson, P. T. Torstensson, E. Kabo, F. Larsson and A. Ekberg. Integrated analysis of dynamic vehicle–track interaction and plasticity induced damage in the presence of squat defects. *To be presented at 10th International Conference on Contact Mechanics* (2015)

All of the papers were prepared in collaboration with the co-authors. The author of this thesis was responsible for the major progress of the work, i.e. took part in planning the papers, developed the computational framework, carried out the simulations and interpreted the results. The dynamic vehicle–track interaction program was developed by Peter Torstensson.

Contents

Part I
Extended Summary

1 Introduction

An introduction to the appended papers is given. Section 1.1 provides a background to the topic, including an overview of previous research within the field. A background to the current research project, its aims and limitations are given in Section 1.2.

1.1 Background

It is not an easy task to give a rigorous definition to the rail surface defects that have become known as "squats". Due to various reasons squats appear and develop somewhat different at different locations under different conditions. The International Union of Railways characterises a squat by "[the] widening and a localised depression of the rail/wheel contact band, accompanied by a dark spot containing cracks with a circular arc or V shape", cf. [25]. Three further characteristics often associated with squats are found in [23]:

- two lung shaped indentations of the rail
- V, U, Y and circular shaped surface breaking cracks
- a widening of the running band

These criteria are rather vague. It might therefore be difficult to tell whether a local indentation of the running band is to be considered as a squat, something that will grow into a squat, or a completely different type of defect. Figure 1.1 may serve as a practical example. This defect has two distinct lobes and a straight surface breaking crack, but does not show any significant widening of the running band. Nevertheless, most people would probably agree that it is a squat. To complicate matters further, it seems to exist (at least) two different kinds of defects that look the same to the naked eye but have different causes and consequences — squats and studs [15]. While the squat is a classical Rolling Contact Fatigue (RCF) kind of defect associated with the accumulation of plastic deformation at the rail surface [14], this is not the case with the stud. Instead, it is considered to be associated with a so-called White Etching Layer (WEL). A WEL is a thin brittle surface layer of the rail material [27]. There are two theories regarding the origin of WEL: 1) phase transformations of the material due to high surface temperatures caused by wheel slip followed by rapid cooling and 2) high rates of shear [14]. Another important difference is that the stud seems to be less prone to cause rail breaks than the squat. In contrast to the squat, which mainly appears on passenger lines and close to the gauge corner of the rail, the stud seems to appear on different types of railways and closer to the middle of the running band [15]. Since the term stud is rather new it is reasonable to assume that some of the "squats" that are reported in the literature are in fact studs.

Figure 1.1: *A defect with two lobes, a straight surface breaking crack but without significant widening of the running band. Photo: Anders Ekberg.*

The defect, which eventually became known as the squat, was found on British railways during the 1970s [14]. However, it turned out that it had been reported on Japanese railways already in the 1950s under the name "black spots" [23]. Due to the risk of transversal crack propagation with possible rail break, the squat gained a lot of attention from the railway community.

During the last decades, efforts have been made to study squat/stud initiation and growth, both experimentally and by numerical simulations. Several metallurgical examinations of squats are found in the literature. One of these actually reports the artificial creation of squats in a twin-disc machine [20]. Other contributions involve simulations of various aspects related to stress intensities of existing squat-type cracks [7, 12, 13]. Studies of this kind mainly focus on existing, rather developed squats.

Although squat-related crack propagation is of great importance, a question that arises, especially from a maintenance point-of-view, is why the cracks initiate in the first place. This is of particular interest for the present work and has previously been studied in a number of articles by the use of transient three-dimensional finite element simulations. In one of the studies, squats that grow from initial surface irregularities are investigated through simulations and field observations [22]. It is stated that the contact forces depend on the local dynamics of the vehicle–track system and that squats that grow from a local irregularity will look more or less the same independently of the initial geometry. However, no explanation is given to the occurrence of the initial irregularities. This study was followed up by another in order to validate the predictions towards field observations [23].

It is claimed that the lung shape of a squat is caused by the dynamic contact force excited by the initial irregularity, which supports the predictions made in [22]. Furthermore it is concluded that numerical studies of squats call for a model that includes a vehicle–track interaction model capable of simulating the high frequency dynamic response.

In another contribution possible sources of the aforementioned initial irregularities are mentioned [21]. These include indentations, bad welds, wheel burns and defects due to wear. By the use of a linear elastic three-dimensional transient FE model, the von Mises stress in the vicinity of differently sized initial irregularities are compared to the material's tensile strength, in order to derive a critical irregularity size. It is suggested that (for the studied conditions) surface irregularities smaller than 6 mm in the lateral and longitudinal directions will be worn away, while irregularities larger than 8 mm are likely to grow into squats. This is reported to correlate well with field observations. Since, most likely, many factors are involved in the process of growing a small irregularity into a squat, the results are probably not generic, although they give a hint on the order of magnitude of the critical size of an initial rail surface irregularity.

Size effects are further investigated in [28]. By studying resulting contact forces of a linear elastic material using a three-dimensional transient FE model, it is concluded that the length, depth and width of a surface irregularity might influence the dynamic contact forces.

The influence of local zones with reduced friction is investigated using a three-dimensional transient FE model in [29]. It is concluded that the shear force reduces in the area of low friction and then increases significantly when nominal friction levels are reached. These results are discussed in connection to squat initiation on tracks without material defects.

1.2 Aim and scope of research

The following work has been performed within the CHARMEC project MU31 — "Squats in rails and RCF clusters on wheels". The overall purpose of the project is to increase the understanding of squats in rails and RCF clusters on wheels by use of numerical simulations. The key aims, originating from the project plan, are summarised below:

- Parametric influence of operational parameters on magnitudes of wear, plastic deformation and crack propagation at local surface irregularities and how this influences the formation of RCF clusters and squats. In particular the plastic deformation, crack formation and growth from local indentations will be studied in detail.

- Influence of the WEL on the state of stress and the propensity for crack growth at a squat. The study should focus on under which conditions (e.g. identification of important operational parameters) a WEL may form and how these influence further crack formation and growth.

- Quantification of dynamic loads and contact stresses at a discrete irregularity on the wheel tread or on the railhead. The increased load magnitude should be compared to typical scatter in operational loads and material strength. The aim is to see at which irregularity magnitudes loads are significantly increased as compared to "natural variations". In particular, the influence of the different dynamic load contributions on crack formation and wear will be investigated in detail. The analysis should feature simulations of high-frequency dynamic vehicle–track interaction. The simulations of the dynamic loading (and contact stresses) should be combined with detailed FE-analyses to derive the resulting stress–strain fields.

The results presented in this thesis cover several of these key aims. The influence of operational parameters on squat initiation is investigated using a high-frequency dynamic vehicle–track model accounting for dynamic loads as well as local contact stresses in the vicinity of local indentations (dimples) and rail corrugation. Detailed FE-analyses (where plastic deformations are taken into account) are used to evaluate the dynamic loads using sophisticated RCF evaluation methods. Even though most of the results are likely to apply also to RCF clusters on wheels as well, such have not been explicitly studied. Furthermore, the main focus in the present thesis is on crack initiation rather than propagation.

2 Dynamic vehicle–track interaction in the presence of surface defects

Beginning in the early 1970s, several so-called multibody dynamic simulation packages have been developed for studies of the vehicle–track dynamics. Well known softwares include ADAMS, GENSYS, NUCARS, SIMPACK and VAMPIRE [3]. The softwares often provide a wide range of analysis alternatives.

Even though many of the normal operating scenarios of rail–vehicle interaction can be described by quasi-static analyses, there are situations where this simplification is not sufficient and the full dynamic response must be resolved. An example of this, which is of particular interest in the current work, is dynamic wheel–rail contact forces and stresses developed due to excitation from rail surface irregularities.

The appended papers utilises the method of moving Green's functions to solve the dynamic vehicle–track interaction response. Therefore, an overview of this method is provided below. In addition, the use of transient FE modelling is discussed to provide a comparison.

2.1 Method of moving Green's functions

The convolution integral method, also known as the Duhamel integral method, is used to compute the dynamic response of linear systems subjected to general load histories. The concept is demonstrated in the subsequent example, which follows [9], where also a rather extensive background is provided.

For illustration, a system with one translational degree-of-freedom (DOF), $u(t)$, describing the position of a mass m attached to a spring with stiffness k is considered. The system is subjected to an impulse acting during the time t_d

$$I = \int_0^{t_d} p\,(t)\,dt \tag{2.1}$$

where t is the time and $p(t)$ is the force. If the mass is initially at rest the equation of motion and its initial conditions can be stated as

$$m\ddot{u} + ku = \begin{cases} p(t), & 0 \leq t \leq t_d \\ 0, & t > t_d \end{cases} \tag{2.2}$$

$$u\,(0) = \dot{u}\,(0) = 0 \tag{2.3}$$

where $\dot{u}$ and $\ddot{u}$ are the first and second time derivatives of the displacement, respectively. Integrating Equation (2.2) over the interval $0 \leq t \leq t_d$ gives the following relation

$$m\dot{u}\,(t_d) + ku_{\mathrm{avg}}t_d = I \tag{2.4}$$

where u_{avg} is the the average displacement. If $t_d \to 0$ then

$$m\dot{u}\left(0^+\right) = I \tag{2.5}$$

which yields the following initial conditions for interval $t > t_d$ of Equation (2.2)

$$\begin{cases} \dot{u}\,(0^+) = \frac{I}{m} \\ u\,(0^+) = 0 \end{cases} \tag{2.6}$$

Solving the resulting differential equation gives

$$u\,(t) = \frac{I}{\omega_{\mathrm{n}} m} \sin\left(\omega_{\mathrm{n}} t\right) \tag{2.7}$$

where $\omega_{\mathrm{n}} = \sqrt{\frac{k}{m}}$. The unit impulse response, also known as a so-called Green's function, denoted $G\,(t)$, is obtained by putting $I = 1$

$$G\,(t) = \frac{1}{m\omega_n} \sin\left(\omega_n t\right) \tag{2.8}$$

Equation (2.8) describes how a suspended mass will oscillate due to a unit impulse acting over a short time. This result can be exploited when the mass is subjected to an entire load history. The impulse due to a load $p\,(\tau)$ acting during the small time interval $d\tau$ is written as

$$dI = p\,(\tau)\,d\tau \tag{2.9}$$

Using Equation (2.7) and (2.9), the displacement increment at time point t due to the load applied at time τ becomes

$$du\left(t\right) = \frac{dI}{m\omega_{\mathrm{n}}}\sin\left(\omega_{\mathrm{n}}\left(t-\tau\right)\right) = p\left(\tau\right)G\left(t-\tau\right)d\tau \tag{2.10}$$

where identification of the ratio appearing in Equation (2.8) is used in the last equality. The total displacement response at an arbitrary time point t is obtained by summing the contributions of all impulse responses from the previous time steps

$$u\left(t\right) = \int_0^t p\left(\tau\right)G\left(t-\tau\right)d\tau \tag{2.11}$$

In this example, the Green's function $G\left(t-\tau\right)$ was derived for the case of an undamped 1-DOF system. However, Equation (2.11) represents a general (as long as the superposition principle holds) expression for how the dynamic response can be obtained. For more complicated systems, like a track model consisting of beam elements resting on discrete springs and dampers, the Green's functions are not derived analytically. Instead Frequency Response Functions (FRF), i.e. functions describing the response in one point of the dynamic system due to a harmonic excitation at another point, are computed in a standard manner using the system matrices of an FE model. The Green's functions can then be obtained by computing the inverse Fourier transform of the FRF [24].

The idea employed in the appended papers is to extend the use of Green's functions to evaluate the dynamic response beneath a wheel moving along a track. To this end the concept of moving Green's functions is introduced [24]. For simplicity a homogeneous rail is henceforth considered although the concept can easily be extended to involve discrete sleeper support. A general Green's function, which is allowed to vary both in time and along the longitudinal coordinate x, is established: $G = G\left(x,t\right)$. The wheel's position is described by $x_p\left(t\right)$ and the wheel–rail normal contact force is denoted $p\left(t\right)$. The rail displacement $w\left(x,t\right)$ due to an applied contact force $p\left(t\right)$, c.f. Figure 2.1, is calculated as

$$w\left(x,t\right) = \int_0^t p\left(\tau\right)G\left(x-x_p\left(\tau\right),t-\tau\right)d\tau \tag{2.12}$$

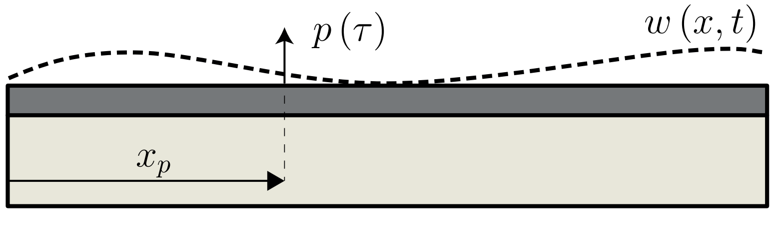

Figure 2.1: *The load $p\left(\tau\right)$ acting at coordinate x_p at time step τ causes the displacement $w\left(x,t\right)$.*

As touched upon previously, the displacement of the track beneath the wheel is typically of primary interest. Therefore it is sufficient to consider the dynamic response at the wheel's current position. This is also the point of excitation. If the wheel is restricted to move only at constant velocity v, the load position at time $t = \tau$ becomes $x_p(\tau) = x_0 + v\tau$, where x_0 is the initial position. Hence, by use of Equation (2.12) the displacement beneath the wheel (indicated by $\sim$) can be expressed as

$$w(x_0 + vt, t) = \widetilde{w}(t) = \int_0^t \widetilde{p}(\tau)\, G(v(t-\tau), t-\tau)\, d\tau \tag{2.13}$$

Since the load history $\widetilde{p}(\tau)$ applied to the wheel, as well as the time difference $t - \tau$ is known, it is possible to evaluate the integral. Note that for a given dynamic system and constant velocity v, the Green's function is a function of the time alone. The moving Green's function $\widetilde{G}_v(t-\tau)$ is now introduced and Equation (2.13) becomes

$$\widetilde{w}(t) = \int_0^t \widetilde{p}(\tau)\, \widetilde{G}_v(t-\tau)\, d\tau \tag{2.14}$$

The moving Green's function $\widetilde{G}_v(t)$ is obtained by considering position $v(t-\tau)$ of $G(x,t)$ at time $t - \tau$. Figure 2.2 schematically illustrates how a moving Green's function $\widetilde{G}_v(t)$ (indicated by the thick solid line) is obtained from a generic Green's function $G = G(x,t)$.

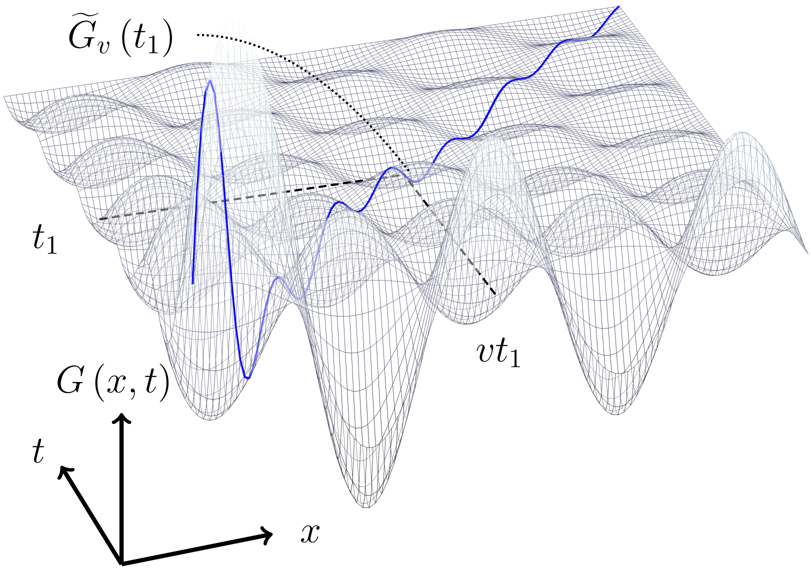

Figure 2.2: *The surface indicates a generic Green's function $G = G(x,t)$ from which the moving Green's function $\widetilde{G}_v(t)$ (marked by the thick solid line) of a point travelling with a constant velocity v is constructed.*

The method of moving Green's functions is implemented in an in-house software for dynamic vehicle–track interaction — RAVEN [5]. Note that the method is not restricted to solve the dynamic response of a track. This is utilised in most of the simulations in the appended papers, where Green's functions are also used to compute wheel displacements. A summary of benefits and drawbacks of the described modelling technique are given below:

+ Pre-calculated Green's functions enable fast simulations.

+ High-frequency dynamic behaviour can be accounted for without adding significant computational costs.

- Only the response of linear systems can be analysed, which means that non-linear characteristics of e.g. ballast (or suspension if modelling the vehicle) is not captured. In contrast, the cause of excitation (in this case the wheel–rail contact force) can be due to non-linear phenomena (in this case the non-linear wheel—rail contact stiffness).

- The trajectory of the contact point needs to be prescribed which makes the modelling technique inappropriate for investigations of low-frequency lateral vehicle dynamics (e.g. stability).

2.2 Transient FE analyses

A transient FE simulation can be used to study the vehicle–track interaction in an integrated manner without any needs for separated sub-modules responsible for the dynamics, contact analysis, continuum stress analysis etc. Furthermore, more realistic (elastic–plastic) wheel–rail material models can be directly incorporated into the analysis. This is particularly useful when it comes to the study of surface irregularities. Examples of studies utilising this technique are given in Section 1.1. Some benefits and drawbacks of this approach are listed below:

+ No need for separate steps in the analysis.

+ No need for approximate theories, such as the elastic half-space assumption used in Hertzian contact theory as well as in CONTACT [19].

- The solution is computationally expensive.

- It might be difficult to perform extensive parametric studies since manual work is often required to update for example the surface geometry.

Even though there are some major advantages with this method, the drawbacks are considered too significant to make it feasible for the purposes of this thesis. However, as the computational capabilities increase, it is likely that the situation will change.

3 RCF evaluation in the vicinity of surface irregularities

Surface initiated RCF stems from the continuous accumulation of plastic strains, i.e. ratchetting, or from low cycle fatigue damage [10]. A proper model for the prediction of RCF initiation of rail surfaces should be able to consider both of these mechanisms. Due to the unconventional load conditions, prediction models for RCF need to fulfill additional requirements compared to conventional fatigue models. As an example, the rail material will experience a multiaxial state of stress with out-of-phase components [10]. This excludes the use of crack initiation models based on uniaxial parameters [26]. The following chapter discusses benefits and drawbacks of some existing RCF initiation/impact models, with special emphasis on their possible applicability in the current study.

3.1 Surface fatigue index

The surface fatigue index, FI_{surf}, was developed as a tool for fast assessment of the risk of surface initiated RCF in combination with the use of e.g. multibody dynamic simulations [11]. Under assumptions of Hertzian contact and full slip conditions, so-called shakedown maps may be constructed [17]. In a shakedown map, a "work point", representing the current loading, is determined by the traction coefficient, the vertical load, the contact geometry and the (cyclic) yield stress of the rail material. An index, FI_{surf}, has been developed to quantify the propensity of surface initiated RCF by calculating the horizontal distance from the current work point to the limiting condition for surface plasticity. It can be shown [11] that the analytical expression of this index becomes

$$FI_{\mathrm{surf}} = f - \frac{2\pi abk}{3F_z} \tag{3.1}$$

where f is the traction coefficient, a and b are semiaxes of the elliptic contact patch, k is the (cyclic) yield stress in pure shear and F_z the vertical load magnitude. Some benefits and drawbacks of the model are listed below.

+ Low computational costs that allow for online implementation in simulations of dynamic vehicle–track interaction.

- Discrete surface irregularities cannot be accounted for since the assumption of Hertzian contact is not fulfilled.

- Only full slip conditions are considered.

- No detailed material response is accounted for.

This RCF impact model is found to be inappropriate for the purposes of the current study since it was not developed to account for discrete surface irregularities.

3.2 $T\gamma$ approach

The idea behind the $T\gamma$ approach is to relate the so-called wear number $T\gamma$, i.e. the sum of the product between the in-plane surface shear force components and their corresponding creepages[1], to fatigue damage. To this end, a damage function has been calibrated against field observations [8]. Some benefits and drawbacks of this model are listed below.

+ Low computational cost that allows for online implementation in simulations of dynamic vehicle–track interaction.
+ Can take the competitive mechanisms between wear and RCF into account.
- No detailed material response is accounted for.
- The approach was not developed to account for surface irregularities.

This RCF impact model is also found to be inappropriate for the purposes of the appended papers since it was not developed to account for discrete surface irregularities.

3.3 Maximum contact stresses and forces

With a sufficiently detailed contact model, such as CONTACT, it is possible to resolve the wheel–rail contact stresses in the vicinity of a surface irregularity. The maximum magnitude of the wheel–rail contact pressure and shear stress, as well as the maximum magnitude of the normal and shear forces then constitute four possible RCF impact measures. Benefit and drawbacks of these very rough RCF impact measures are listed below.

+ The influence of local surface irregularities is accounted for.
- The required contact model is computational demanding (as compared to Hertzian contact).
- No detailed material response is accounted for.
- The method is very rough with no clear link to RCF initiation mechanisms.

This approach is used in **Paper A**.

3.4 Jiang–Sehitoglu fatigue parameter

The Jiang–Sehitoglu fatigue parameter [16] is a multiaxial low cycle fatigue parameter that can be considered to be a combination of energy density and critical plane approaches. This parameter has been employed in FE based predictions of RCF crack initiation in rail heads [26]. It has also been used in relation to railway wheels, e.g. regarding the influence

[1] Creepage can be defined as the ratio of the sliding velocity (between the wheel and rail) and the vehicle speed, cf. [3].

of material defects on RCF [18].

The fatigue parameter is calculated as

$$FP = \max\left\{\left\langle \frac{\Delta\epsilon}{2}\sigma_{\max}\right\rangle + c_{\mathrm{J}}\Delta\gamma\Delta\tau\right\} \tag{3.2}$$

where the maximisation is carried out over all orientations (material planes). c_{J} is a material parameter and $\langle x\rangle = 1/2\left(|x| + x\right)$. Note that the $\langle x\rangle$ notation is not present in [16] but occurs in different forms in the literature, cf. [18, 26]. For a given plane, $\sigma_{\max}$ is the maximum normal stress on the material plane, $\Delta\epsilon$ the normal strain range, $\Delta\gamma$ the engineering shear strain range and $\Delta\tau$ the shear stress range. The engineering shear strain (and stress) range is computed as

$$\Delta\gamma = \max_{t,\bar{\tau}\in C}\left|\boldsymbol{\gamma}\left(t\right) - \boldsymbol{\gamma}\left(\bar{\tau}\right)\right| \tag{3.3}$$

where t and $\bar{\tau}$ are instants in time belonging to the load cycle C and $\boldsymbol{\gamma}$ is the vectorial engineering shear strain of the studied plane. As seen in Equation (3.2), stress and strain fields, typically obtained through FE analyses, are to be provided, which makes a post processing evaluation suitable. Some benefits and drawbacks of the Jiang–Sehitoglu fatigue parameter are

+ It is possible to perform detailed fatigue evaluations.
+ The approach is rather general and implicitly accounts for the influence of local surface irregularities.
- Detailed stress and strain fields, typically obtained at a high computational cost, must be provided.
- It is computationally expensive to calculate the fatigue parameter for all material planes and positions of interest.
- The criterion is local whereas, in reality, fatigue is a "semi-local" phenomenon.

This approach is used in **Paper B** and **C**.

3.5 Equivalent stress and strain

As mentioned above, ratchetting is a common cause for surface initiated RCF of rail heads. This process can be studied by using FE simulations in combination with a material model able to capture non-linear hardening. A straight forward approach is then to compute and assess the stress–strain response in material points of particular interest. To this end, the effective von Mises stress and strain are convenient to use. The von Mises strain can be defined as

$$\bar{\epsilon} = \frac{\sqrt{2}}{3}\sqrt{\left(\epsilon_{xx} - \epsilon_{yy}\right)^2 + \left(\epsilon_{yy} - \epsilon_{zz}\right)^2 + \left(\epsilon_{zz} - \epsilon_{xx}\right)^2 + 6\left(\epsilon_{xy}^2 + \epsilon_{yz}^2 + \epsilon_{xz}^2\right)} \tag{3.4}$$

where ϵ_{ij} is a component of the total strain tensor. Similarly, the von Mises stress is defined as

$$\bar{\sigma} = \frac{1}{\sqrt{2}}\sqrt{\left(\sigma_{xx} - \sigma_{yy}\right)^2 + \left(\sigma_{yy} - \sigma_{zz}\right)^2 + \left(\sigma_{zz} - \sigma_{xx}\right)^2 + 6\left(\sigma_{xy}^2 + \sigma_{yz}^2 + \sigma_{xz}^2\right)} \qquad (3.5)$$

for the components σ_{ij} of the stress tensor. Plotting the von Mises stress against the strain will graphically indicate whether or not a state of shakedown is obtained. Some benefits and drawbacks of this approach are

+ It is possible to perform detailed fatigue evaluations.

+ The approach is rather general and implicitly accounts for the influence of local surface irregularities.

- Detailed stress and strain fields, typically obtained at a high computational cost, must be provided.

- An advanced material model is needed, which increases the computational cost.

- The criterion is local whereas, in reality, fatigue is a “semi-local” phenomenon.

This approach is used in **Paper B** and **C**.

4 Overview of computational model

A computational model to evaluate the influence of operational and geometrical parameters with respect to squat initiation is presented in [5] and summarised in Figure 4.1. It is based on three different modules indicated by a solid border: dynamic vehicle–track interaction analysis, finite element simulation and RCF evaluation. Intermediate results, acting as interfaces between the modules, are highlighted with a dashed border. User input, here in terms of operational parameters, such as velocity, creepage, axle load etc. as well as track surface irregularities are provided to the dynamic module and highlighted by a thin dotted border.

As mentioned in Chapter 2, there are different possibilities regarding the dynamic model. Here, the in-house code RAVEN [5] is employed. Based on the method of moving Green’s functions, cf. Section 2.1, the dynamic response in terms of wheel and rail displacements is computed. An implementation of CONTACT [19] is used to solve the local contact problem. The different modules of the computational model are further described in Section 4.1–4.3.

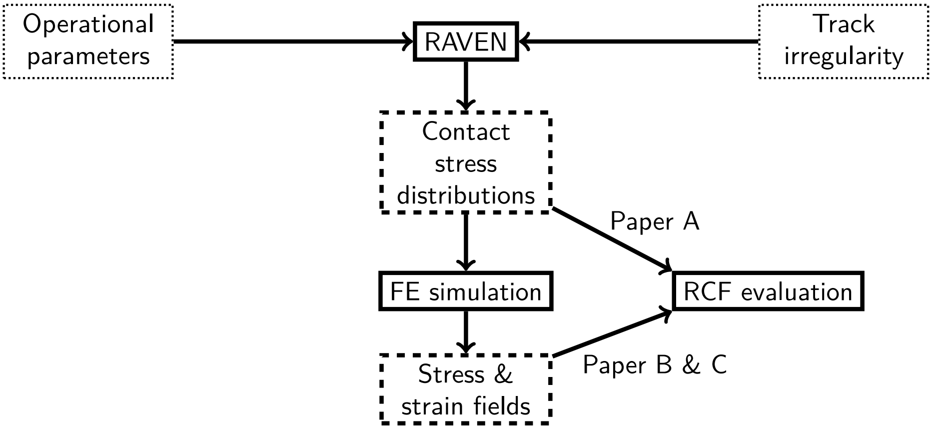

Figure 4.1: *Flow chart showing an overview of the computational model. User input is indicated by a thin dotted border, computational modules by a solid and intermediate results by dashed rectangles.*

4.1 Dynamic model — RAVEN

In RAVEN a vehicle that consists of a wheel hinged on its primary suspension running along a flexible track is simulated. A rigid wheel is considered in most of the simulations. The track model is built up by flexible beam elements supported by springs, dampers and masses calibrated towards the response of an operational track. Here, only vertical dynamics is considered, although there are no theoretical limits to extend the model to account also for three-dimensional dynamics.

Figure 4.2 shows the main evaluation steps of RAVEN. As a preprocessing step, the (moving) Green's functions are calculated for the wheel and the track. The computational efforts of producing the Green's functions of the track are high compared to the typical simulation time. However, for a specific track model and a specific velocity they only have to be calculated once. This is a major benefit of this approach.

The Green's functions are used to compute wheel and track displacements via a convolution integral, cf. Equation (2.11). In some types of analyses (e.g. involving an unsprung wheel or non-linear primary suspension characteristics) it is unsuitable to calculate a Green's function of the wheel. The wheel displacement is then computed using an ordinary differential equation (ODE) solver. The track displacements are however always obtained via a convolution integral. Based on the displacements of the wheel and track it is possible to determine the wheel–rail normal pressure and shear stress distributions using CONTACT. Note that even if the wheel most often is considered as rigid in the dynamic simulation, this is not the case when solving the local contact problem. Due to the half-space assumption both bodies are assumed to have linearly elastic properties. Furthermore, both two-dimensional and three-dimensional contact situations can be treated although only two-dimensional vertical dynamics is considered. The calculated stress distributions are saved for postprocessing and resulting contact forces serve as an input to the convolution integral solution for the next time step. This procedure continues until the simulation is finished. Contact stress distributions as well as resulting contact forces are saved to be used as inputs for the FE simulations, cf. Figure 4.1.

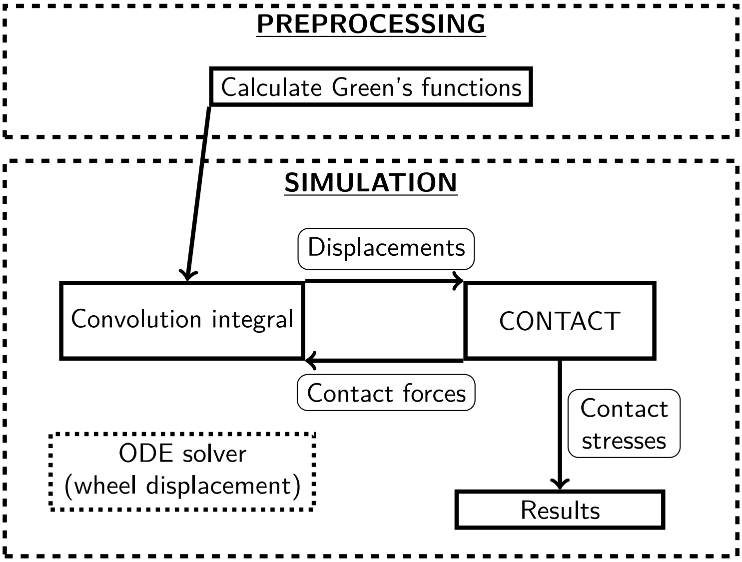

Figure 4.2: *Flow chart showing the main steps of RAVEN.*

4.2 FE simulations

The contact stress distributions obtained from RAVEN are mapped onto the surface of an FE domain representing a section of the rail supported by rollers, cf. Figure 4.3. Note that the load, which moves over the surface using the same step size as employed in RAVEN, is not restricted to either Hertzian pressure distributions or full slip conditions.

The detailed stress–strain response is obtained for all time steps considered. When the desired number of load cycles have been obtained, the stress–strain history is exported for RCF evaluation. In this thesis, the rail section is represented by a 300 × 100 mm plane strain body modelled in the commercial FE code ABAQUS [1]. A built-in material model that features non-linear kinematic and isotropic hardening is calibrated towards the first five load cycles (which is also the number of wheel passages considered in the simulations) of a real rail material subjected to cyclic loading [2]. Furhter details are given in **Paper B** [5].

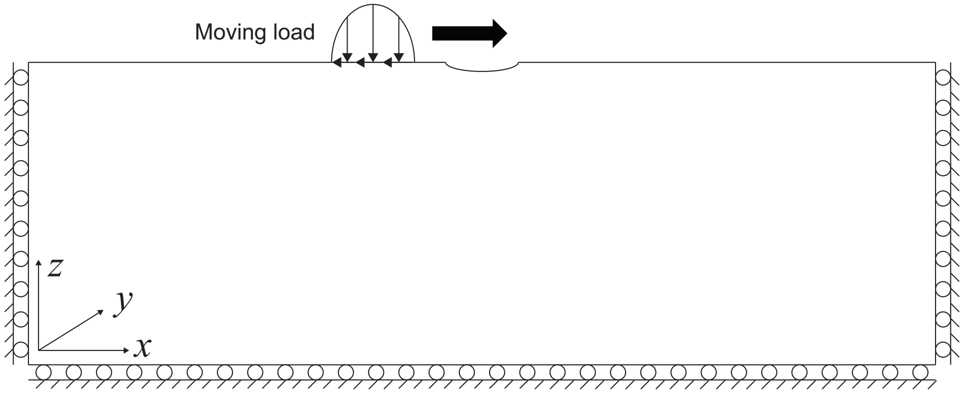

Figure 4.3: *Schematic view of the FE model consisting of a rail section. Boundary conditions and a moving load is outlined. Note that the load is not restricted to either a Hertzian contact distribution or full slip conditions.*

4.3 RCF evaluation

Evaluated stress-strain histories from the FE simulations are input variables for the assessment of RCF impact. Here the Jiang–Sehitoglu fatigue parameter as well as the accumulated strain are considered, cf. Sections 3.4 and 3.5.

4.4 Modelling assumptions

The computational model uses several assumptions and simplifications. Some of these, as well as potential consequences, are listed below.

- Only vertical dynamics is considered. This means that phenomena associated to lateral dynamics, such as hunting motions [3] cannot be studied. This modelling assumption is justified for operations on tangent track in cases where the lateral dynamics is not of primary interest.
- The use of (moving) Green's functions in RAVEN requires that both the vehicle and track models are linear. Hence, non-linear characteristics e.g. of vehicle suspension and ballast cannot be captured.
- CONTACT is based on the elastic half-space (half-plane in two dimensions) assumption. Any influence of an elastic–plastic material response on contact stresses are thus not taken into account. Furthermore, the half-plane assumption is violated in the vicinity of dimple irregularities. The dimple geometry has been made smooth in the appended papers, partly in order to minimise the influence of this issue.

- Both CONTACT and the FE simulations are based on quasi-static conditions. The dynamic effects are thus taken into account to determine the structural response in RAVEN, but not explicitly accounted for when local contact stresses as well as rail material responses are evaluated.

- Only two-dimensional FE simulations are performed. Differences in response between two-dimensional and three-dimensional contact evaluations have been investigated in **Paper A**. These indicated that results are expected to be qualitatively similar [6]. Although an extrapolation to state that the qualitative similarity extends also to results from FE simulations would be premature, there are no indications of the opposite.

5 Summary of appended papers

5.1 Paper A: The influence of rail surface irregularities on contact forces and local stresses

The effect of initial rail surface irregularities on promoting further surface degradation is investigated. The study considers RCF formation, in particular in the form of squats. The impact of surface irregularities of dimple types is quantified by peak magnitudes of dynamic contact stresses and contact forces, cf. Section 3.3. To this end, two-dimensional (later extended to three-dimensional) RAVEN simulations are employed, i.e. the first step of the analysis chain shown in Figure 4.1. The most influencing parameters are identified. It is shown that even very shallow dimples might have a large impact on local contact stresses. Peak magnitudes of contact forces and stresses due to the influence of the studied rail dimples are shown to exceed those due to three studied cases of rail corrugation.

5.2 Paper B: An efficient approach to analyse rail surface irregularities accounting for dynamic train–track interaction and inelastic deformations

A two-dimensional computational model for assessment of RCF induced by discrete rail surface irregularities — especially in the context of squats — is presented. The idea is to follow the entire analysis chain presented in Figure 4.1. Dynamic excitation in a wide frequency range is considered by the use of RAVEN. Results from dynamic simulations are mapped onto an FE model to resolve the cyclic elastic–plastic stress response in the rail. Strain accumulation during five wheel passages is quantified. In addition, low cycle fatigue impact is quantified using the Jiang–Sehitoglu fatigue parameter, as described in Section 3.4. The functionality of the model is demonstrated by numerical examples.

5.3 Paper C: Integrated analysis of dynamic vehicle–track interaction and plasticity induced damage in the presence of squat defects

The computational model described in **Paper B** and shown in 4.1 is used to study some interesting operational scenarios identified in **Paper A**. It is seen that the RCF impact (both in terms of accumulated strain and fatigue parameter magnitude) will increase with the size of the surface irregularity. Furthermore, it is shown that the coefficient of friction constitutes a decisive parameter in the presence of surface dimples. It is also seen that clustering of rail surface irregularities might have a large impact on RCF. The influence of varying friction conditions is studied by considering a rail with a nominal coefficient of friction of 0.5, which is lowered to 0.1 at a 30 cm long rail section before the nominal value is retained. The accumulated strain in the vicinity of the low friction section is found to be low compared to in the vicinity of surface dimples although the fatigue parameter is in the same order as for a small dimple.

6 Conclusions, main results and future work

The present thesis treats surface initiated RCF of rails, especially in the context of squats. By use of a numerical simulation scheme summarised in Figure 4.1, the influence of various parameters believed to influence RCF crack initiation are investigated. Main results and conclusions from the study are discussed in the present chapter.

The maximum wheel–rail normal pressure and interfacial shear stresses as well as maximum resulting normal forces and shear forces (which all constitute rough measures of RCF impact) in the presence of surface irregularities are studied. The maximum magnitudes of shear stresses and shear forces are found to be highly affected by friction and creepage. The maximum normal pressure only shows a significant dependence of the geometry of the irregularity (i.e. length and depth). Vehicle speed and irregularity positions (relative to a sleeper) only have a considerable influence on the maximum normal force. Also very shallow dimples give large impact on maximum normal pressure and shear stress in the wheel–rail contact. Comparisons towards three-dimensional wheel–rail contact analyses show strong qualitative similarities, although absolute magnitudes differ.

Two lightly and one severely corrugated rail are also compared against the RCF impact obtained by local rail surface irregularities. It is concluded that in most of the studied cases, discrete surface irregularity defects result in higher magnitudes of forces and stresses than severe corrugation.

Combined dynamic and FE-analyses show that RCF impact increases with the size of a surface dimple and that clustering of dimples may play an important role. Furthermore it is shown that the coefficient of friction is a very important parameter, both in connection to dimples, but also if it varies rapidly on a smooth rail.

Possible consequences on squat initiation are listed below:

- In the case of a discrete surface irregularity, the size will be important. The larger the initial irregularity the larger the propensity for squat initiation.
- Clusters of surface irregularities might play an important role in the promotion of squat initiation.
- Discrete rail surface irregularities are likely to be more prone to initiate squats than rail corrugation.
- The friction conditions between wheel and rail are important. The RCF impact due to recovery of partial slip from a state of full slip conditions may be in the same order as that obtained by a small surface irregularity.

A lot of open questions regarding squat initiation remain unanswered. Some important tasks that are left as future work are listed below:

- As mentioned in Section 1, it has been suggested that WEL might play an important role in squat (stud) initiation. There is a need for further investigations on the influence of WEL in the context of squat initiation.
- Fully developed squats are associated with complex crack networks beneath the rail surface. Since these cracks might propagate and cause rail fractures (local or global), it is of interest to analyse the crack response due to dynamic loads.
- Real world squats develop in three dimensions. To capture possible associated effects, an extension from two- to three-dimensional (FE) simulations is needed.
- It has not yet been fully shown that the studied RCF impact measures are relevant for squat initiation predictions. The research would benefit from validation of numerical results towards experiments.

References

[1] *Abaqus v. 6.12-1.* Computer Program. 2012.

[2] J. Ahlström and B. Karlsson. Fatigue behaviour of rail steel - A comparison between strain and stress controlled loading. *Wear* **258**.7-8 (2005), 1187–1193. DOI: 10.1016/j.wear.2004.03.030.

[3] E. Andersson, M. Berg, and S. Stichel. *Rail Vehicle Dynamics.* Stockholm: KTH, 2014. 342 pp. ISBN: 978-91-7595-420-2.

[4] R. Andersson et al. Integrated analysis of dynamic vehicle–track interaction and plasticity induced damage in the presence of squat defects. *To be presented at 10th International Conference on Contact Mechanics* (2015).

[5] R. Andersson et al. An efficient approach to analyse rail surface irregularities accounting for dynamic train–track interaction and inelastic deformations. *Submitted for international publication* (2015).

[6] R. Andersson et al. The influence of rail surface irregularities on contact forces and local stresses. *Vehicle System Dynamics* **53**.1 (2015), 68–87. DOI: 10.1080/00423114.2014.982890.

[7] S. Bogdański and M. W. Brown. Modelling the three-dimensional behaviour of shallow rolling contact fatigue cracks in rails. *Wear* **253**.1-2 (2002), 17–25. DOI: 10.1016/S0043-1648(02)00078-9.

[8] M. C. Burstow. *Whole Life Rail Model Application and Development for RSSB – Continued development of an RCF damage parameter*. Report. Rail Safety and Standards Board, 2004. 65 pp.

[9] R. R. Craig and A. J. Kurdila. *Fundamentals of Structural Dynamics*. Second Edition. Hoboken, New Jersey: John Wiley & Sonc, Inc., 2006. 728 pp. ISBN: 978-0-471-43044-5.

[10] A. Ekberg and E. Kabo. Fatigue of railway wheels and rails under rolling contact and thermal loading - an overview. *Wear* **258**.7-8 (2005), 1288–1300. DOI: 10.1016/j.wear.2004.03.039.

[11] A. Ekberg, E. Kabo, and H. Andersson. An engineering model for prediction of rolling contact fatigue of railway wheels. *Fatigue and Fracture of Engineering Materials and Structures* **25**.10 (2002), 899–909. DOI: 10.1046/j.1460-2695.2002.00535.x.

[12] M. Farjoo et al. Stress intensity factors around a 3D squat form crack and prediction of crack growth direction considering water entrapment and elastic foundation. *Engineering Fracture Mechanics* **94** (2012), 37–55. DOI: 10.1016/j.engfracmech.2012.07.011.

[13] D. I. Fletcher. Numerical simulation of near surface rail cracks subject to thermal contact stress. *Wear* **314**.1-2 (2014), 96–103. DOI: 10.1016/j.wear.2013.11.021.

[14] S. L. Grassie. Squats and squat-type defects in rails: The understanding to date. *Proceedings of the Institution of Mechanical Engineers, Part F: Journal of Rail and Rapid Transit* **226**.3 (2012), 235–242. DOI: 10.1177/0954409711422189.

[15] S. L. Grassie et al. Studs: A squat-type defect in rails. *Proceedings of the Institution of Mechanical Engineers, Part F: Journal of Rail and Rapid Transit* **226**.3 (2012), 243–256. DOI: 10.1177/0954409711421462.

[16] Y. Jiang and H. Sehitoglu. A model for rolling contact failure. *Wear* **224**.1 (1999), 38–49.

[17] K. L. Johnson. The strength of surfaces in rolling contact. *Proceedings of the Institution of Mechanical Engineers.Pt.C.Journal of Mechanical Engineering Science* **203** (1989), 151–163. ISSN: 0954-4062.

[18] E. Kabo and A. Ekberg. Material defects in rolling contact fatigue of railway wheels - The influence of defect size. *Wear* **258**.7-8 (2005), 1194–1200. DOI: 10.1016/j.wear.2004.03.070.

[19] J. J. Kalker. *Three-dimensional elastic bodies in rolling contact*. Vol. 2. Dordrecht: Kluwer, 1990. 314 pp. ISBN: 9780792307129; 0792307127.

[20] M. Kaneta et al. A possible mechanism for rail dark spot defects. *Journal of Tribology* **120**.2 (1998), 304–309.

[21] Z. Li, X. Zhao, and R. Dollevoet. “The Determination of a Critical Size for Rail Top Surface Defects to Grow into Squats”. *8th Int. Conference on Contact Mechanics and Wear of Rail/Wheel Systems*. Vol. 2, pp. 379–388.

[22] Z. Li et al. An investigation into the causes of squats - Correlation analysis and numerical modeling. *Wear* **265**.9-10 (2008), 1349–1355. DOI: 10.1016/j.wear.2008.02.037.

[23] Z. Li et al. Squat growth - Some observations and the validation of numerical predictions. *Wear* **271**.1-2 (2011), 148–157. DOI: 10.1016/j.wear.2010.10.051.

[24] A. Pieringer. *Time-domain modelling of high-frequency wheel/rail interaction.* Göteborg: Chalmers tekniska högskola, 2011. 107 pp. ISBN: 978-91-7385-523-5.

[25] *Rail defects*. 4th edition. UIC Code 712. Paris: International Union of Railways, 2002. 107 pp. ISBN: 2-7461-0341-9.

[26] J. W. Ringsberg. Life prediction of rolling contact fatigue crack initiation. *International Journal of Fatigue* **23**.7 (2001), 575–586. DOI: 10.1016/S0142-1123(01)00024-X.

[27] M. Steenbergen and R. Dollevoet. On the mechanism of squat formation on train rails - Part I: Origination. *International Journal of Fatigue* **47** (2013), 361–372. DOI: 10.1016/j.ijfatigue.2012.04.023.

[28] X. Zhao, Z. Li, and R. Dollevoet. The vertical and the longitudinal dynamic responses of the vehicle–track system to squat-type short wavelength irregularity. *Vehicle System Dynamics* **51**.12 (2013), 1918–1937. DOI: 10.1080/00423114.2013.847466.

[29] X. Zhao et al. A study on high-speed rolling contact between a wheel and a contaminated rail. *Vehicle System Dynamics* **52**.10 (2014), 1270–1287. DOI: 10.1080/00423114.2014.934845.